Applied Acoustics 74 (2013) 1–9

Contents lists available at SciVerse ScienceDirect

Applied Acoustics

journal homepage: www.elsevier.com/locate/apacoust

An experimental and numerical study of blast induced shock wave mitigation in sandwich structures

Benjamin Schimizze [a,*], Steven F. Son [b], Rahul Goel [c], Andrew P. Vechart [d], Laurence Young [e]

[a] School of Mechanical Engineering, Purdue University, West Lafayette, IN 47907, USA
[b] Department of Mechanical Engineering, Purdue University, West Lafayette, IN 47907, USA
[c] School of Aeronautics and Astronautics, Massachusetts Institute of Technology, Cambridge, MA 02139, USA
[d] Computation for Design and Optimization Program, Massachusetts Institute of Technology, Cambridge, MA 02139, USA
[e] Department of Biomedical Engineering, Massachusetts Institute of Technology, Cambridge, MA 02139, USA

ARTICLE INFO

Article history:
Received 26 July 2011
Received in revised form 12 May 2012
Accepted 28 May 2012
Available online 17 August 2012

Keywords:
A. Shock waves
B. Finite elements
C. Inhomogeneous material
D. Acoustics
E. Blast mitigation

ABSTRACT

The liners of US military helmets are typically made using common soft foams. In order to better protect troops from Traumatic Brain Injury resulting from Improvised Explosive Devices, it is necessary to better understand the material properties involved in air blast mitigation. In this work, mitigation properties are studied using sandwich samples made from a vinyl-nitrile foam shell filled with materials which were selected to span a range of material properties. These materials—water, glycerin, glass beads, Aerogel®, CAB-O-SIL®, tuff volcanic rock, and expanding foam—were compared to both uniform vinyl-nitrile foam and a US Army helmet pad. Possible modes of shock attenuation include inertial effects based on density and acoustic impedance, dispersion based on porosity, and thermal effects. Since no standard test exists, we developed two experimental configurations to evaluate performance. The results were additionally used to verify a numerical model made using ABAQUS® software. Both the numerical model and the experimental results were consistent in showing that most materials attenuate the peak blast pressure while Aerogel® actually enhances the blast. Density and acoustic impedance mismatch are shown to be of primary importance while porosity is shown to have an effect as well. Furthermore, a differentiation is made between reflective and absorptive shock mitigation.

1. Introduction

Traumatic Brain Injuries (TBIs) resulting from explosions represent a significant percentage of military personnel injuries. According to the Defense and Veterans Brain Injury Center [3], more than 150,000 US military personnel have been medically diagnosed with a Traumatic Brain Injury (TBI) since 2001 [25]. Severity of TBIs ranges from mild injuries to head penetration injuries. Wojcik et al. reported that 46.7% of TBIs in subjects from Operation Enduring Freedom (OEF) in Afghanistan and 63.9% of TBIs in subjects from Operation Iraqi Freedom (OIF) in Iraq were attributable to exposure to explosions. In contrast to previous conflicts, improved body armor enabled personnel to survive TBI-causing experiences that were previously fatal. Furthermore, the understanding and recognition of TBIs has recently improved in the medical community, leading to a higher rate of diagnosis. The increased use of Improvised Explosive Devices (IEDs) has raised the probability of exposure of personnel to TBI-causing explosions [23].

This project addresses the need for improved protection against primary blast-related TBI resulting from explosively generated shock waves. As an extension of previous work on fluid helmet liners for sports, new combat helmet liner strategies are being developed that would add blast protection to the capabilities of the standard issue helmet, supplementing the current protection from other injuries. The essential new element is the inclusion of moveable or deformable materials, sandwiched within foam, to dissipate the blast energy, reduce the peak transmitted pressure, and broaden the blast waveform before it reaches the brain.

The objectives for this study are as follows:

(1) Develop experimental strategies to test the mitigation potential of different materials.
(2) Test material combinations.
(3) Compare experimental results to the results of numerical modeling.

* Corresponding author. Address: 4220 Bramble Ave., Apt. 3, Cincinnati, OH 45227, USA. Tel.: +1 614 288 8195.
E-mail addresses: bschimizze@gmail.com (B. Schimizze), sson@purdue.edu (S.F. Son), rahulg@mit.edu (R. Goel), avechart@mit.edu (A.P. Vechart), lry@mit.edu (L. Young).

0003-682X/$ - see front matter © 2012 Elsevier Ltd. All rights reserved.
http://dx.doi.org/10.1016/j.apacoust.2012.05.011

2. Materials

2.1. Fluid-filled composite materials

The concept of incorporating fluid within channels in helmets is not new. Morgan [13] proposed a plurality of inter-connected expandable chambers with valves, placed inside the helmets. These chambers would be filled with non-compressible fluid. Upon impact, the fluid would be displaced from the first chambers to empty second chambers, and would be returned back to the first chamber after the impact force is removed. In the last four decades there have been many attempts [2,6,9,10,21,12] to employ air bladders or fluid chambers; however, none of the proposed concepts fully materialized and none of the approaches are directly applicable to the blast protection problem. Ponomarev and Ponomaryova [15] describe a method for placing a partially evacuated chamber filled with air or another gas between the blast source and the object to be protected, including the body. The chamber ruptures under the incoming pressure peak and the relative vacuum absorbs the ambient air, creating a negative pressure wave to interfere with the positive wave from the blast and reduce the transmitted pressure. Stuhmiller et al. [20] suggested a cushion for use in body armor to mitigate shock loads. It may include numerous fluid pockets that could be deformable or reconfigurable, and are therefore connected to empty reservoir pockets. Transport of fluid was allowed through a vent controlled by a valve.

Stewart [19] showed the effectiveness of channels filled with glycerin mixtures in reducing the transferred impact forces by viscous dissipation and by compression of foam. These foam samples were made of high energy absorbing foam made of vinyl nitrile manufactured by Der-Tex Corporation. The same foam type was used in the present study as well.

There has been limited research on use of filler materials in body armors. Gerber et al. [5] and Groves and Groves [7] suggested the use of compressible materials in the form of glass beads for use in body armor. Rhoades et al. [17] suggested use of a shear thickening material made of polyborosiloxane for sports padding, bulletproof vests, weaponry etc.

2.2. Primary blast mitigation

Blast injury mechanisms are generally categorized at five different levels, the first (primary blast effects) of which is the focus here. Primary effects are direct damage caused by gas overpressure. According to Schardin [18], primary effects can be further divided into three areas: spallation, implosion, and inertia. Spallation occurs when a blast wave propagates from a higher density medium to a lower density medium; this creates fragmentation of the higher density medium. Implosion, sometimes referred to as cavitation, is the result of rapid pressurization of gases within tissues which then expands with enough kinetic energy to create damage. Inertial, or impact, injuries are the result of shear stresses and fast accelerations. Primary effects can cause concussion-like symptoms, which include memory dysfunction and cognitive deficits, and have been associated with post-traumatic-stress disorder [24].

Most experimental work on blast mitigation has been done with kilogram-scales of explosives with direct contact between the explosive and the mitigating material. While these types of experiments are useful in understanding general blast wave phenomena, they are not likely to be directly applicable towards personal protection from shock waves. For example, in survivable air shocks the pressure is less than 100 psi (689.5 kPa) while pressures near the surface of an explosive are orders of magnitude higher. Nevertheless, the results of these works were considered in designing the shock wave experiments, and they will factor into the conclusions and discussion.

2.3. Filler materials

Different material properties have been suggested to provide blast attenuation. Depending on the acoustic impedance of the interacting medium, the shock wave will reflect, transmit, and dissipate to differing degrees. Zhuang et al. [26] examined scattering effects of stress waves in layered composite materials. The large impedance mismatches at the interfaces created longer rise times for the shock front, essentially increasing the time for a maximum stress to be obtained under a given loading condition. The timescale of the stress will determine how effectively the stress wave couple to the tissues. A computational study by Li and Meng [11] examined the effect of multiple internal interfaces on dissipation and dispersion effects through the cellular media. Cellular collapse at low velocity impacts was verified to attenuate energy transfer effects. However, Nesterenko [14] suggests that certain porous materials could actually amplify the peak pressure of the shock wave, so choice of materials is critical.

Wakabayashi et al. [22] conducted experiments that suggest that low-density materials may provide the most effective blast mitigation. These experiments were conducted with direct contact between the explosive and the mitigant in a confined fashion. Materials studied were water gel, polystyrene spheres, combinations of gel and spheres, and natural silica sand. Hartman et al. [8] investigated the mitigation capabilities of foams over a range of expansion ratios. Contradictory to previous studies, they conclude that the mid-range expansion ratios (and thus densities) were optimal for mitigation purposes.

Allen et al. [1] studied the attenuation effects of water, sand, glycerin, grade P25 and P05 expanded perlite, and porous water which was made using micro-sized balloons. They concluded that density is of primary importance in addition to porosity. Thermal effects were shown to be negligible. Gel'fand et al. [4] investigated water mitigation in confined explosive experiments and concluded that the thermal effects of water are insignificant to blast attenuation while inertial effects dominate waters mitigation capabilities. Resnyansky and Delaney [16] further investigated water mitigation in a similar fashion but also included water in the form of mist. Most studies involving these suggest that the total mitigant mass is a significant factor in overall attenuation.

It can be concluded from these studies that density, total mass, and porosity play an important role in blast mitigation; although their precise application and optimization has yet to be realized. Further, air blast mitigation has received far less attention compared to direct contact explosives. In order to test each of these proposed strategies, experiments were designed and conducted to measure free field air blast parameters from an unconfined, unobstructed explosive charge. Subsequent experiments were then performed with the various materials sandwiched in foam samples and subjected to blast loading.

3. Experimental design

Explosive testing was performed using an explosively driven shock tube (Fig. 1). The distance between shock wave and blast products is increased compared to a free field blast while preserving most of the total energy of the shock because the shock wave and blast products are constrained to a single direction. In addition, the pulse width produced is made similar to a large explosive with a charge that is placed farther away. Two, 5 in. (12.7 cm) inner diameter, steel, cylindrical sections are separated by steel blast plates of thickness 0.5 in. (2.54 cm) into two chambers, the detona-

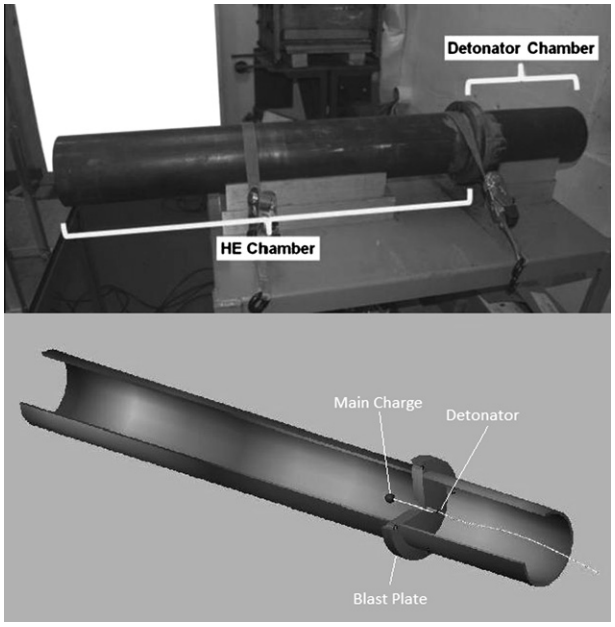

Fig. 1. Picture (top) and drawing (bottom) of explosively driven shock tube.

tor chamber and the high explosive (HE) chamber. The chambers are bridged together with a 1 in. (2.54 cm) diameter hole in the connecting blast plates.

Explosions were initiated using one Teledyne RISI RP-502 exploding bridge wire (EBW) detonator placed in the fore section of the detonator chamber. The RP-502 is equivalent to a #8 blasting cap and is encased in aluminum that creates shrapnel upon detonation. The test object is protected from the shrapnel by the previously mentioned blast plate. The detonation is then bridged between chambers using 6 in. (15.24 cm) of PETN detonation cord which is knotted and extends 2 in. (5.08 cm) beyond the blast plate into the HE chamber. Each test used three grams of Primasheet 1000 by Ensign-Bickford Aerospace & Defense (EBA&D). Primasheet 1000 is a plasticized high explosive containing 63% PETN nominally. The Primasheet is shaped around the knotted detonation cord into a sphere. The resultant shock wave and explosion are directed towards the testing apparatus by the tube.

No standard test exists to study the attenuation of air blasts by mitigation materials. Two different test apparatuses were developed and used, the second being a refinement of the first. The first apparatus used a testing stand with an open frame structure constructed from 1 in. angle aluminum mounted to an optical table (Fig. 3). On the front of the structure, a sample holder was attached that secured the sample in a vertical position with the front face perpendicular to the axis of the blast. A Plexiglas® chamber was attached to the back of the sample in order to minimize the effect of the shock wave coming around the test sample. The chamber was constructed using 0.25 in. × 16 in. × 7.5 in. (6.35 × 406.4 × 190.5 mm) Plexiglas®

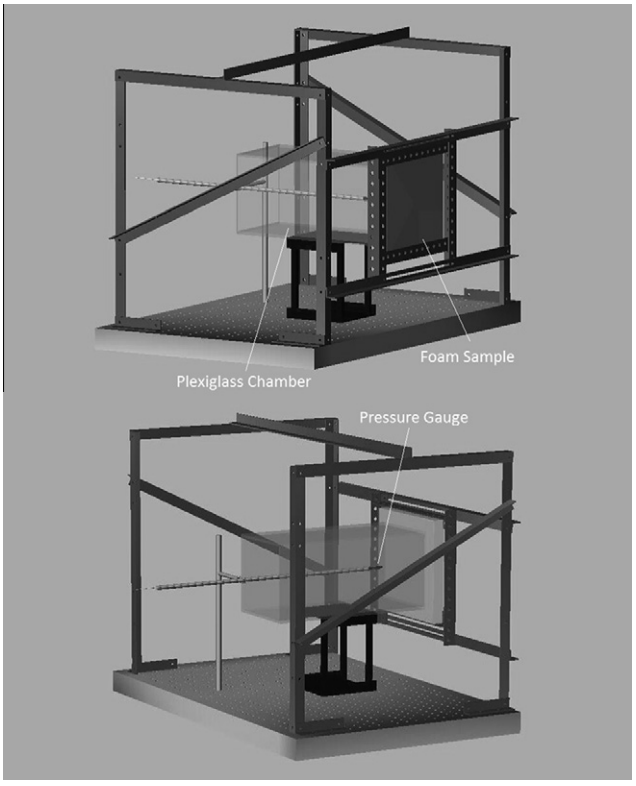

Fig. 3. Initial test apparatus with isolation chamber, pressure gauge, and sample.

panels. The back end was left open to allow placement of the pressure sensor. Samples were placed between two 0.125 × 10 × 10 in. (3.175 × 254 × 254 mm) Plexiglas® sheets in order to maintain the structure of the foam samples. The front face of the Plexiglas® was located 12 in. (30.48 cm) in front of the mouth of the shock tube, and a single PCB 113A22/113B22 dynamic pressure sensor was placed behind the sample at a distance of 2.75 in. (69.85 mm) behind the back face of the sample making the stand off distance between the mouth of the shock tube and the pressure sensor 16 in. (40.64 cm). The pressure sensor was aligned with the axis of the blast in order to eliminate off-axis effects. A schematic of this configuration can be seen in Fig. 2.

In order to house a variety of mitigating materials, sandwich foam samples were constructed. The control material used was vinyl-nitrile VN-600 foam manufactured by Der-Tex Corporation. The foam is characterized by the company as a microcellular, energy-absorbent foam with a density ranging from 95 kg/m^3 to 120 kg/m^3. The control sample was a solid foam sample of size 10 × 10 × 1 in. (254 × 254 × 25.4 mm). Variable samples consisted of the same outer control foam with a single-cavity removed core of size 8 × 10 × 0.5 in. (203.2 × 254 × 12.7 mm). The cavity was then filled and sealed. See Fig. 4 for a diagram of the sample configuration.

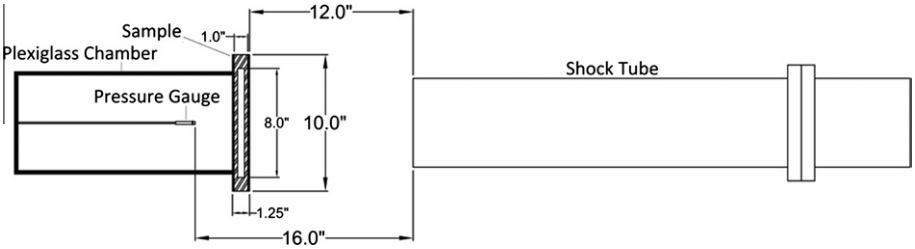

Fig. 2. Top view schematic of Plexiglas® chamber configuration.

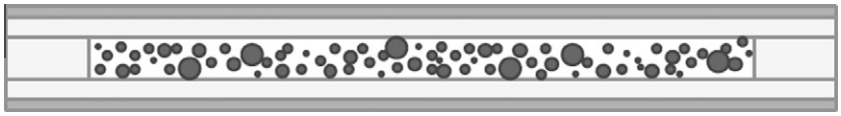

Fig. 4. Cutaway diagram of the sample configuration.

Table 1
Mechanical and acoustic properties of different filler materials.

Filler material	ρ (kg/m^3)	Particle size (μm)	C_o (m/s)	Z_o (103 kg/m^2 s)	Viscosity (Pa s)
Water	1000	n/a	1500	1500	0.0009
Glycerin	1260	n/a	1900	2400	1
Aerogel®	5–200	1000–5000	70–1300	10	n/a
CAB-O-SIL®	35–60	0.2–0.3	100–1500	5–100	n/a
Glass beads	2456–2486	250–420	3700–5300	10,000	n/a
Expanding foam	1060	n/a	Unknown	Unknown	n/a
Tuff	1300	n/a	Unknown	Unknown	n/a

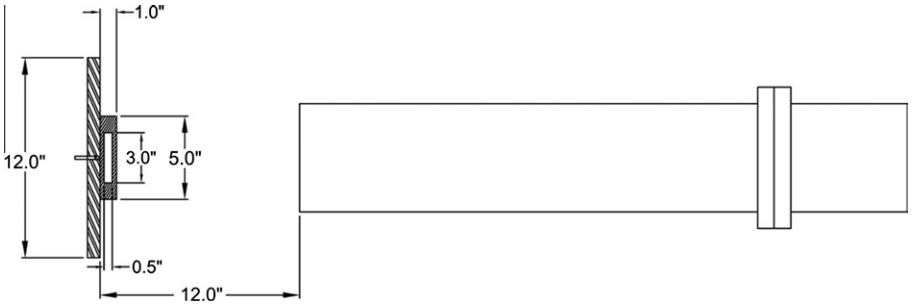

Fig. 5. Top view schematic of aluminum plate configuration. From left to right: aluminum plate with embedded pressure gauge, sample with cavity, and shock tube.

Filler materials were selected in order to span a range of possible attenuating features particularly viscosity, density, and particle size. Water and glycerin have similar mechanical/acoustic properties but their viscosity varies by four order of magnitude. Particle size was varied among three of the loose solid filler materials, Aerogel®, CAB-O-SIL®, and glass beads. Density was varied among filler materials also. Aerogel® and CAB-O-SIL® represent low density materials; water, glycerin, and expanding spray foam represent medium density materials; and glass beads and tuff volcanic rock represent high density materials. Refer to Table 1 for properties of the filler materials.

The first test configuration required a Plexiglas™ sheet on both sides of the sample in order to maintain structural integrity of the sample and to keep the pad from impacting the gauge. This resulted in a large portion of the blast wave being reflected off of the front Plexiglas™ sheet as evidenced by the low pressures transmitted and the results of shadowgraphy. The second test apparatus used an aluminum plate configuration (Figs. 5 and 6). A single pressure sensor was embedded in an aluminum plate measuring $0.75 \times 12 \times 6$ in. ($19.05 \times 304.8 \times 152.4$ mm). The gauge was recessed 2 mm from the surface of the plate and coated with vacuum grease in order to transmit the shock wave. The size of the sample was reduced for sampling. The new dimensions of the samples were $5 \times 5 \times 1$ in. ($139.7 \times 139.7 \times 25.4$ mm), and the new dimensions of the cavity were $5 \times 3 \times 0.5$ in. ($139.7 \times 76.2 \times 12.7$ mm). All orientations from the initial configuration were maintained. The standoff distance between the front of the aluminum plate and the mouth of the shock tube was 12 in. (30.48 cm).

CAB-O-SIL® was eliminated from the second test design because it was very similar to Aerogel® mechanically. Tuff and expanding foam were eliminated because their material properties were partly unknown, and they did not perform well in the first test configuration. A pad taken out of an Army Advanced Combat Helmet (ACH) was added for comparison; however its exact properties are unknown.

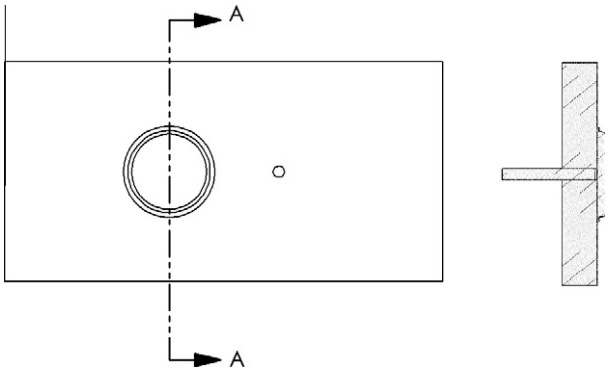

Fig. 6. Schematic of aluminum plate configuration with embedded pressure gauge and circular sample.

4. Numerical modeling

Air blast loading on flat sandwich samples used in the experiments is simulated in ABAQUS®/Explicit using the built in CONWEP module. The equivalent mass of TNT for the explosive and the point of detonation need to be specified in the module. The equivalent

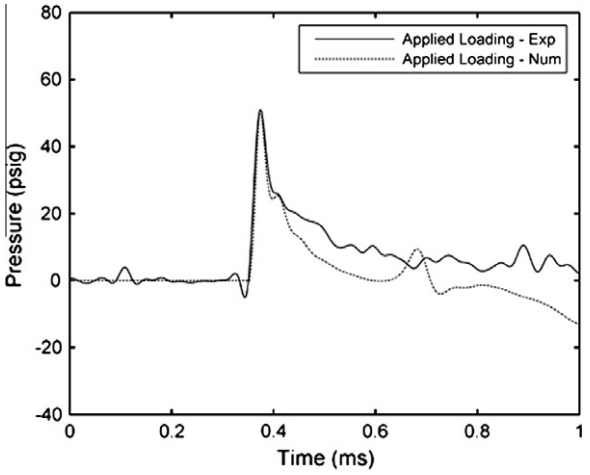

Fig. 7. Comparison of applied loading on front face of the sample.

mass of PETN used was 2.87 g. This accounts for the Primasheet® and detonating cord. The distance of detonation of the explosive was carefully selected in the model so that the loading applied on the front face matches that of the experimental loading. The point of detonation was chosen as 11.75 in. (29.84 cm) in front of the sample. At this distance, the peak pressure generated by the module is 51 psig (352 kPa) when fluid–structure interaction effects are considered. In the experiments, the peak pressure of the applied loading at 11 in. (27.94 cm) in front of the shock tube is also 51 psig (352 kPa). There is good agreement of applied loading between the experiments and the simulations as seen in Fig. 7. However, positive duration and thus impulse (time integral of pressure) are slightly lower for the numerical loading as compared to experimental. The same loading was applied for all the test cases simulated.

Flat sandwich structure samples as shown in Fig. 8 are modeled in ABAQUS®. Development of a numerical model to observe the response of the foam liner coupled with a model of the Army's Advanced Combat Helmet (ACH) and human head model is currently under way.

There are two different approaches used to model the flat plate structure: one for solid filler material and another for fluid filler material. The flat plate structure for solid filler material is treated as one solid block with different sections having different properties. The overall dimensions of the sandwich plate structure are $5 \times 5 \times 1$ in. ($12.7 \times 12.7 \times 2.54$ cm), similar to that in the experiments. A cavity of size $5 \times 3 \times 0.5$ in. ($12.7 \times 7.62 \times 2.54$ cm) is modeled as in the experimental samples. Properties of filler materials can be assigned to this region. Foam and the solid filler materials are modeled using Lagrangian elements. In order to simulate the benchmark case, i.e. pure foam samples, the fill region (Fig. 8a) can be assigned the material properties of foam. The structure lies parallel to the X–Y plane, and the blast source is 11.75 in. (29.84 cm) vertically above (along the z-direction) the center of the top face of the structure.

Initially, the structure is in its undeformed state. The back surface of the sandwich structure is fixed for all degrees of freedom. The four sides of the structure are assigned zero surface forces. The plate surface is discretized using $51 \times 51 \times 10$ C3D8R elements, i.e. 8-node linear brick elements with reduced integration and hourglass control. The primary parameter of interest is the transmitted pressure. Solutions are computed up to 1 ms after detonation of the explosive. Uniaxial stress–strain data obtained from high strain rate testing using split Hopkinson bar is used for the foam material. The linear shock-Hugoniot relation:

$$U_s = C_o + sU_p \tag{1}$$

is used to model the filler materials where C_o and s are material dependent constants. This is used in conjunction with the Mie-Grüneisen equation of state,

$$P = \frac{\rho_o C_b^2 \eta}{(1 - s\eta)^2} \cdot \left(1 - \frac{\Gamma_o \eta}{2}\right) + \Gamma_o \rho_o e \tag{2}$$

where ρ_o is reference density, $\eta = 1 - \rho/\rho_o$, Γ_o is the Grüneisen parameter, and e is the internal energy per unit mass. Table 2 gives the material properties used for modeling.

Shear modulus is used to model solid fillers while dynamic viscosity is used to model liquids. Analysis for fluid filler materials (water and glycerin) is performed using the coupled Eulerian–Lagrangian (CEL) method in ABAQUS®/Explicit. The solid foam is modeled using Lagrangian elements, whereas the fluid is modeled using Eulerian elements. The Eulerian implementation is based on the volume-of-fluid method. In this method, the material is tracked as it flows through the mesh by computing its Eulerian volume fraction (EVF). If a material completely fills an element, its EVF is one; if no material is present in an element then its EVF is zero. The flat plate (foam sample) is modeled with a cavity as shown in Fig. 8b. The fluid domain (Fig. 8c) is slightly extended on the front side of the foam and has a thickness of 1.25 in. (3.175 cm). Eulerian elements residing within the cavity are assigned an initial EVF of 1, and the rest are assigned an EVF of 0. Dynamic viscosity is also included in the material model for fluid filler materials to model the shear response. The dynamic viscosity, μ, for water at $T = 20$ °C is 0.001 Pa s, whereas that for glycerin is 1.5 Pa s.

The back surface of the solid domain is fixed for all degrees of freedom. The four sides of the solid domain are assigned zero surface forces. The two sides of the fluid domain corresponding to the openings of the cavity are assigned zero velocity in normal direction in order to constrain the fluid within the cavity. The solid domain is discretized in the same manner as earlier, whereas the fluid domain is discretized using $118 \times 118 \times 25$ EC3D8R elements, i.e. 8-node linear Eulerian bricks. Reduced integration is used with vis-

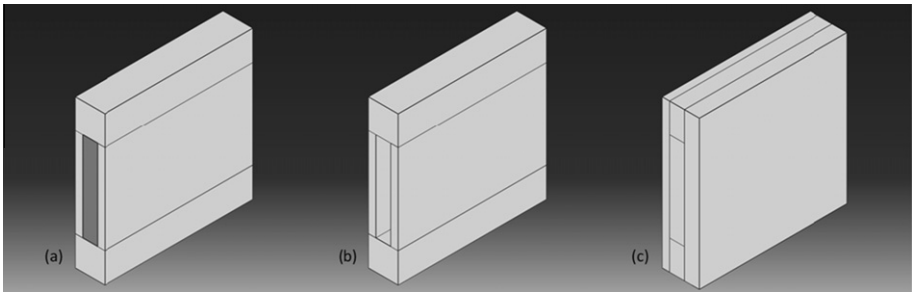

Fig. 8. (a) Flat plate model for solid fillers; (b) flat plate model for fluid fillers – Lagrangian part; (c) flat plate model for fluid fillers – Eulerian part.

Table 2
Material properties used in numerical model.

Material	Density, ρ (kg/m^3)	Shear modulus, G (GPa)	Poisson ratio (v)	Bulk sound velocity c (m/s)	Material constant (s)
Foam	108	0.000405	0.33	108.44	1.35
Glass beads	1460	30.4	0.226	2010	1.8
Aerogel®	94.7	0.00417	0.2	567	1.0833
Water	1000	n/a	n/a	1490	1.92
Glycerin	1260	n/a	n/a	1900	1.6

Table 3
Initial tests, results are averaged over two tests.

Sample	Pulse duration (ms)	Peak pressure (psig)
Free-field	1.13	15
Solid foam	1.27	0.86
CAB-O-SIL®	0.98	0.98
Aerogel®	1.14	0.91
Expanding foam	1.42	0.8
Tuff	1.31	0.56
Glass beads	1.68	0.47
Water	1.53	0.57
Glycerin	1.58	0.45

cous hourglass control. Solutions are computed up to 2 ms after detonation, where transmitted pressure values appear to have stabilized. Dynamic analysis in double precision using ABAQUS®/Explicit is carried out.

5. Results and discussion

5.1. Experimental results

The results for the initial configuration are presented in Table 3. The initial mitigation experiments show large attenuation for every sample; however, distinctions can be made among the materials. The largest factor in the attenuation by the material of peak pressure was the density. High density materials reduced the peak pressure from between 33% and 48% when compared to the control sample. The lowest density materials showed even less attenuation than the control sample. Additionally, higher density materials seemed to increase the pulse duration in general.

The overall attenuation for each material was more than 93%. Shadowgraph (Fig. 9) imaging revealed that a large portion of the wave was reflecting off of the front surface of the Plexiglas®. Because the Plexiglas®, and multiple interfaces, had such a large effect, plate test results were used to corroborate the initial results.

The results are shown in Table 4. The plate experiments are similar to the initial results but were more conclusive. The reference pressure for a free field blast at this distance, 12 in. (30.48 cm) is 90 psig. Density was again very important. The densest materials (i.e. water, glycerin, and glass beads) had the best mitigation of peak pressure in general; however, glass beads—the densest material—showed less attenuation than both water and glycerin. A likely explanation for this is that glass beads are discontinuous while water and glycerin are continuous; the air gaps between beads could provide a path of transmission for the shock wave.

The lower density materials showed less attenuation, and Aerogel® actually showed a magnification of the peak pressure which is consistent with Nesterenko [14]. It is possible that the wave speed

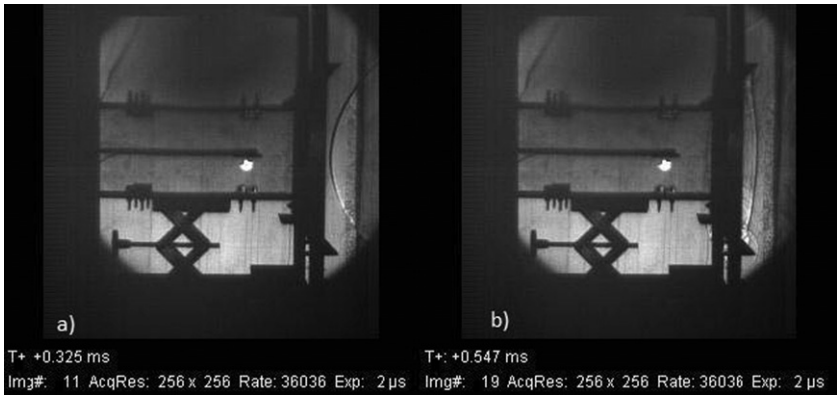

Fig. 9. Shadowgraphy results for control sample of solid foam in the initial test setup. (a) Shows the incoming shock wave. (b) Shows the shock wave reflecting off the Plexiglas® surface of the test configuration.

Table 4
Statistical results of peak pressure and impulse/area.

Material	Mean peak pressure (psig)	Pulse duration (ms)	Standard error (psig)
Free field	94.33	0.41	3.45
Water	31.91	0.57	1.56
Glycerin	32.81	0.65	1.6
Glass beads	54.22	0.61	2.65
Solid foam	74.17	0.42	2.72
Army pad	74.48	0.55	3.64
Aerogel	99.32	0.42	3.64

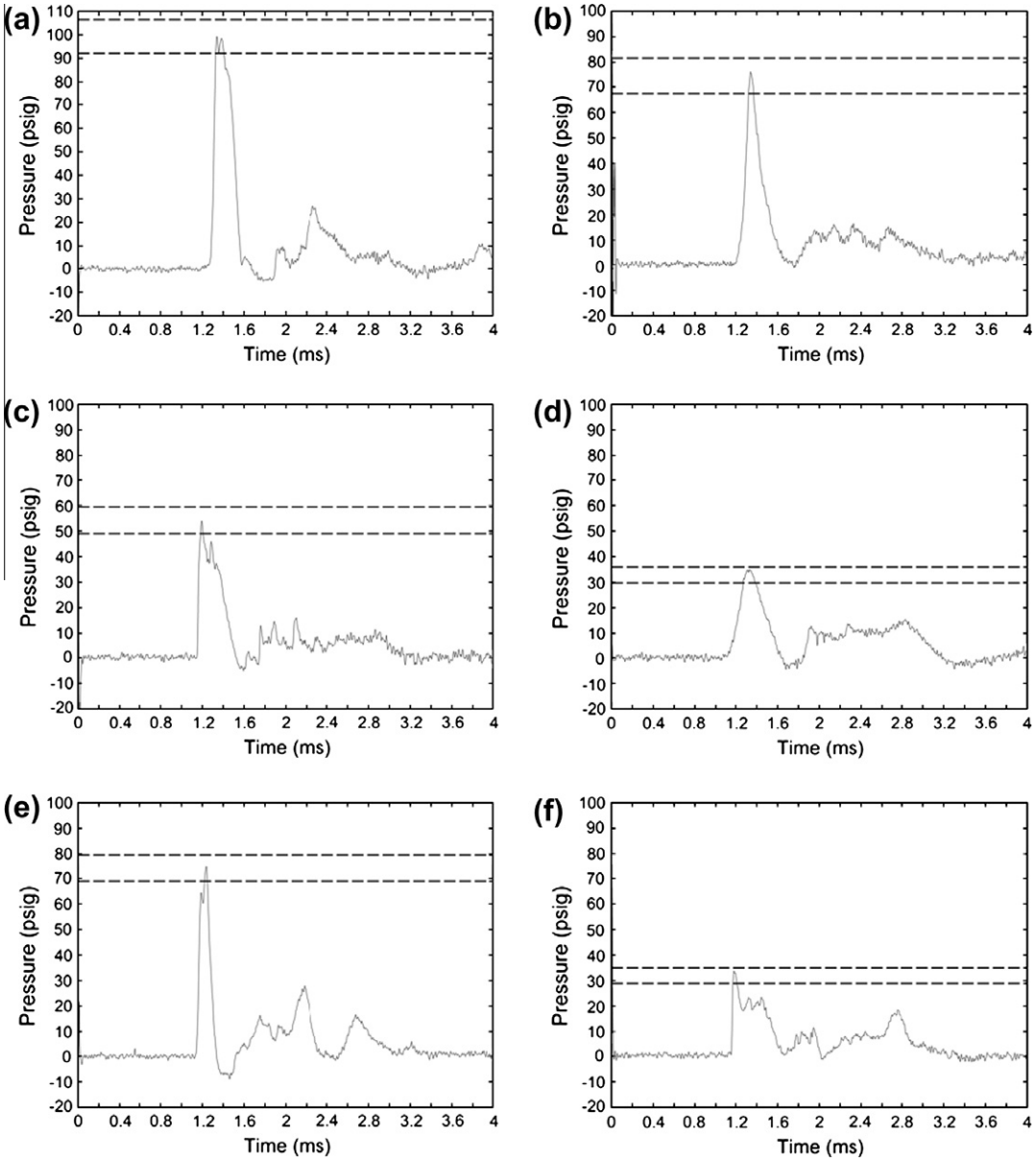

Fig. 10. Typical transmitted pressure of (a) Aerogel®, (b) Army pad, (c) glass beads, (d) glycerin, (e) Der-Tex foam, and (f) water. Error bars set at 95% confidence interval.

and pressure increased as a result of entering a material denser than air, but almost none of the shock wave was reflected due to the extremely low impedance and density of Aerogel®. Furthermore, Aerogel® powder was a loose material and contributed less resistance to the crushing force of the pressure wave. This was not the case with the Army pad and solid foam which were connected porous solid materials. The density of the solid Der-Tex foam was low at 108 kg/m^3. The mode of attenuation for these two materials, Der-Tex and the Army pad, was likely absorptive rather than reflective.

A way to imagine this is with a simple dynamic system of a mass with a spring and dashpot on both sides with an applied force. For the three low density materials, the mass is low and the spring constant is high. The difference is that the dashpot damping for the Aerogel® is negligible while it is medium for the foam materials. The energy absorption is the result of either stretching or tearing of the solid parts of the materials upon pore collapse. This example can be extended to the high density materials where the mass in the dynamic system is high. A significant portion of the applied force will be resisted or reflected by the high mass; however, there is no significant method of energy absorption, so the dashpot damping is negligible.

When considering the application of these materials in helmets, energy absorption is much more desirable than energy reflection because the Kevlar® helmet itself provides substantial reflective protection from shock waves; however, shock waves can bend around the edge of the helmet and travel between the helmet and skull. At this point, purely reflective materials would do little to dissipate the transmitted wave while absorptive materials would have a greater effect.

While materials reduced the level of peak pressure, they also shaped the shock waves and pressure traces to consistent forms. Pressure traces are presented in Fig. 10 below. Reference lines are set at 95% confidence interval for peak pressure. Aerogel®, which had almost no effect on the peak pressure, also had nearly zero effect on the shape of the wave. The peak pressures behind so-

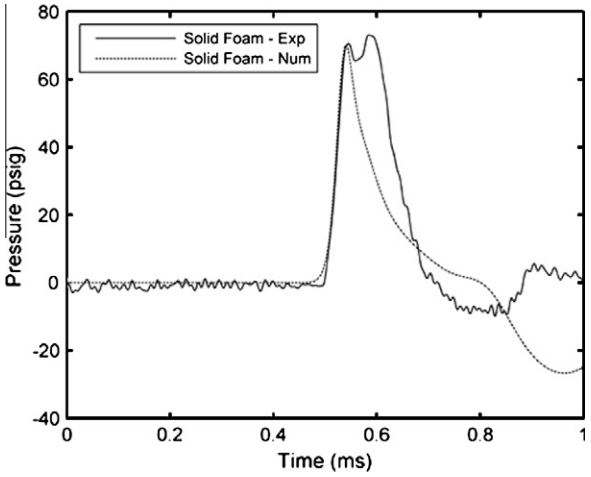

Fig. 11. Comparison of transmitted pressure behind solid foam sample.

Table 5
Comparison of experimental and numerical results.

Sample	Experimental pressure results (psig)	Numerical pressure results (psig)
Solid foam	74.1	70.5
Aerogel®	99.3	50.5
Glass beads	54.2	34.0
Water	31.9	35.0
Glycerin	32.8	31.5

lid Der-Tex foam and behind the Army foam pad were nearly identical; however, the Army foam pad causes the pulse width to double. Glass beads, glycerin, and water all caused the pulse width to widen. The rise time of the initial peak is also important. Glycerin and the Army pad showed the most effect in this sense while the other materials did not significantly affect the rise time.

The reason for the different shapes of the traces for the different materials—Army foam for instance has a smooth peak, while water has many peaks—is the acoustic interaction of the shock wave with macroscopic structure of the material. It is expected that small glass beads would affect the wave differently than the lower density porous foams, i.e. Army pad and Der-Tex, and the ultra-low density Aerogel® which keep the shape of the peak relatively consistent. The glass beads show a multiple peaking effect.

Water and glycerin, which showed roughly the same mitigation of peak pressure, had a very different response. Of all the materials, water's shaping of the wave was most significant while glycerin did not change the shape of the peak except by widening of the pulse width some. Water and glycerin have similar densities, and the main difference between them is their viscosity which may have a large effect on the transmission of the shock wave.

5.2. Comparison with numerical models

The model is validated against the experimental results for the solid foam benchmark case. Peak transmitted pressure is the primary parameter of interest. Fig. 11 shows a comparison of transmitted pressure measured behind the foam sample at the center of the sample both experimentally as well as in the simulations. The results are tabulated in Table 5. A good agreement between the experiments and the model can be observed, especially for peak pressure and rise time. The average peak pressure for three trials during the experiment was roughly 74.17 psig (511 kPa) with a standard error of 2.72 psi (18.75 kPa) whereas peak pressure observed numerically is 70.5 psig (485 kPa). There is some discrepancy in the time duration, but this could be an artifact of the discrepancy in time duration of the loading profile.

The timing (~0.02 ms) of the two peaks observed for the case of solid foam in experiments is indicative of a local complexity in the shock wave. The numerical model uses a simplified planar wave while the actual shock wave has a spherical front which becomes further convoluted by material interactions. The circular corner to the gauge recess is the likely cause for the second peak as the only localized, high impedance non-uniformity; although this is inconclusive. Nonetheless the second peak represents an experimental artifact inherent to extremely dynamic systems.

The numerically calculated pressure traces recorded behind the sample for solid filler materials and fluid filler materials are shown in Fig. 12a and b, respectively. The peak pressure calculated for glass beads was 34 psig (234.5 kPa), which is a nearly 50% reduction over solid foam. Also, glass beads showed a high pressure plateau, which was partially seen in some experiments. Rise time and time duration for glass beads were markedly higher than the solid foam control case. The peak pressure calculated for Aerogel® was 50.5 psig (348 kPa), which is nearly a 30% reduction over solid foam. These results are in partial agreement with the experiments. Glass beads also have nearly three orders of magnitude higher impedance than Aerogel®. Another possible source of incongruence between the model and experiment beyond peak pressures is the pressure gauges. The pressure gauges used are piezo-electric which are dynamic is design. They become less accurate with increasing time because the change bleeds off, and gage pressures are refer-

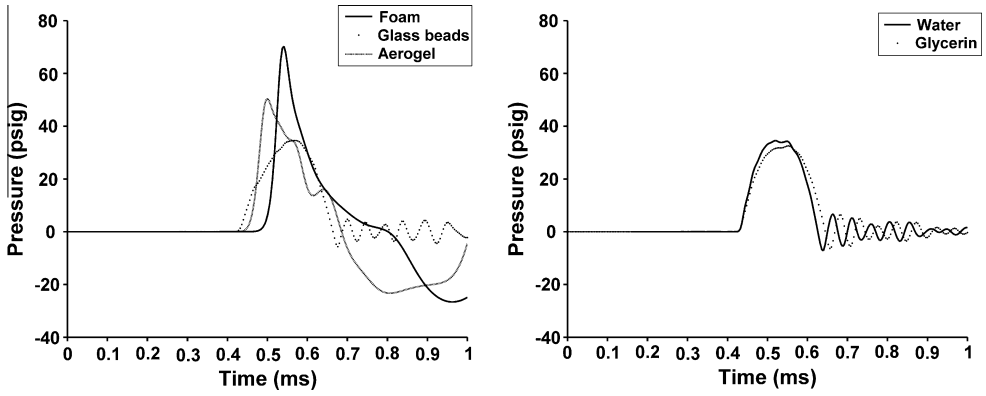

Fig. 12. Comparison of transmitted pressure for (a) solid fillers; (b) liquid fillers.

enced to ambient conditions; this may play a role in the results. Fig. 12b shows the calculated response of the liquid fillers – water and glycerin. The water pressure trace has a peak of 35.0 psig (241.5 kPa) whereas that of glycerin is 32.5 psig (224 kPa). Glycerin also shows a slightly longer rise time and longer time duration compared to water.

6. Summary and conclusion

In this investigation of blast mitigation by sandwich samples, numerical modeling was used to calculate the pressure response for two different test configurations. The samples were a combination of Der-Tex foam and several different filler materials including water, glycerin, glass beads, and Aerogel®. Samples were subjected to blast loading by an explosively driven shock tube at a standoff distance of 12 in. The experimental goal was to specifically look at the attenuation of the shock wave as opposed to all primary blast effects. A model was developed using ABAQUS®/Explicit which was verified with the blast experiments.

The results of experimentation and modeling lead to the following conclusions:

(1) Density and impedance are of primary importance when considering a material's ability to mitigate an air shock wave. For high density materials, which include water, glass beads, and glycerin, the mode of mitigation is reflective which is not ideal for helmet padding.
(2) Low density, porous materials which include the Army helmet pad and Der-Tex foam, showed an ability to attenuate the wave. The mode of mitigation here is absorptive and a result of stretching and/or tearing of the solid material surrounding a collapsing pore. This mode of attenuation is more ideal for helmet padding.
(3) The shock wave strength was amplified by Aerogel®. This was due to Aerogel's® low overall density and impedance along with the fact that it was a loose material. This phenomenon has also been seen in certain porous materials in previous work.
(4) Materials showed an ability to predictably shape the incoming shock wave in most cases. Glycerin and the Army pad showed the biggest increase in rise times, and the Army pad, glass beads, glycerin, and water caused an increase in pulse width.
(5) Numerical models were successful in predicting the peak pressure results of the blast experiments especially in regards to relative attenuation among materials with the exception of Aerogel®.

Acknowledgements

Authors are thankful to the financial support provided by Office of Naval Research (#N00014-08-1-0261) and Deshpande Center at MIT.

We would like to thank the previous graduate students, Matt Alley and George Christou. We would also like to thank professors at MIT (Radovitzky, R; Socrate, S; and Gibson, L.) who helped in technical discussions and material testing.

References

[1] Allen RM, Kirkpatrick DJ, Longbottom AW, Milne AM, Bourne NK. Experimental and numerical study of free-field blast mitigation. In: Furnish MD, editors. Proceedings of shock compression of condensed matter. Portland, OR: AIP Conference Proceedings; 2003.
[2] Calogne R, Fluidos SL. Resistant Helmet Assembly. US Patent 5815846; 1998.
[3] DVBIC, Defense and Veterans Brain Injury Center. <http://www.dvbic.org>; 2010 [accessed 25.05.2010].
[4] Gel'fand BE, Sil'nikov MV, Mikhailin AI, Orlov AV. Attenuation of blast overpressures from liquid in an elastic shell. Combust, Explo, Shock Waves 2001;37(5):607–12.
[5] Gerber U, Gerber E, Hofer P, Fischer E, Lusuardi W, Gysel W, Baggi R, Rogg E, Gutt K. Armor and a method of manufacturing it. US Patent 4665794; 1987.
[6] Gooding ER. Energy-absorbing insert for protective headgear. US Patent 4375108; 1983.
[7] Groves TK, Groves D. Body armor. US Patent 5087516; 1992.
[8] Hartman WF, Boughton BA, Larsen ME. Blast mitigation capabilities of aqueous foam. Sandia National Laboratories, SAND2006-0533; 2006.
[9] Holt MC. Tomczak WF. Protective gear with hydraulic liner. US Patent 3849801; 1974.
[10] Hosaka. Helmet and fluid reservoir system. US Patent 5148950; 1992.
[11] Li QM, Meng H. Attenuation or enhancement – a one-dimensional analysis on shock transmission in the solid phase of a cellular material. Int J Impact Eng 2002;27:1049–65.
[12] Mendoza ID. Safety helmet. US Patent 6560787; 2003.
[13] Morgan GE. Energy absorbing and sizing means for helmets. US Patent 3609764; 1971.
[14] Nesterenko VF. Shock (blast) mitigation by "soft" condensed matter. In: MRS Symp Proc; 2003. p. 759.
[15] Ponomarev V, Ponomaryova I. Blast compression wave absorbing device. US Patent 7017705; 2006.
[16] Resnyansky AD, Delaney TG. Experimental study of blast mitigation in a water mist. WeaponsSystemsDivision. Defense Science and Technology Organisation, DSTO-TR-1944; 2006.
[17] Rhoades LJ, Matechen JM, Rosner MJ. Smart Padding system utilizing an energy absorbent medium and articles made there from. US Patent 6701529; 2004.
[18] Schardin H. The physical principles of the effects of a detonation. German aviation medicine. World War II. Washington, DC: Department of the US Air Force, Office of the Surgeon General; 1950. p. 1207–24.
[19] Stewart D. A protective helmet liner incorporating fluid channels. MS Thesis, Dublin: UCD School of Electrical, Electronic and Mechanical Engineering; 2008.
[20] Stuhmiller JH, Chan P, Stuhmiller L. Anti-blast and shock optimal reduction buffer. US Patent 250548; 2008.
[21] Villari FK, Steigerwald CJ, Rappleyea FA. Protective helmet. US Patent 3994021; 1976.
[22] Wakabayashi TH, Matsumura T, Nakayama Y. Reduction of explosion damage using sand or water layer. Shock Compress Condens Matter; 2007.
[23] Warden D. Military TBI during the Iraq and Afghanistan Wars. J Head Trauma Rehab 2006;21:398–402.
[24] Wolf Stephen J, Bebarta Vikhyat S, Bonnett Carl J, Pons Peter T, Cantrill Stephen V. Blast injuries. Lancet 2009;374:405–15.
[25] Wojcik BE, Stein CR, Bagg K, Humphrey RJ, Orosco J. Traumatic brain injury hospitalization of U.S. Army soldiers deployed to afghanistan and iraq. Am J Prev Med 2010;38:S108–16.
[26] Zhuang S, Ravichandran G, Grady DE. An experimental investigation of shock wave propagation in periodically layered composites. J Mech Phys Sol 2003;51:245–65.